COMPUTATIONAL STUDY OF STATE RELATIONSHIPS FOR ACETYLENE-AIR DIFFUSION FLAMES WITH SOOT RADIATION

Z. Zhang and O.A. Ezekoye
Department of Mechanical Engineering
University of Texas at Austin
Austin, Texas

ABSTRACT

Time history effects are suspected to affect the dynamics of soot evolution within heavily sooting non-premixed flames. The majority of soot chemistry calculations have been conducted for steady flame configurations. In this study, the combustion processes for a spherical acetylene-air diffusion flame element are computed using two fundamentally different approaches. In the first case, the state relationship data from experiments are used to specify the major gas species distributions, while in the second case, a finite rate reaction mechanism is used. A simplified soot mechanism which incorporates the effects of soot nucleation, surface growth, oxidation and agglomeration processes is used to specify the soot species evolution. It is found that as the net radiative losses for the diffusion flame element approach zero, the predictions of the state relationships match the results from the finite rate calculations.

NOMENCLATURE

a_p Planck mean absorption
a, b, c, d exponent constants in the reaction rate expressions
A pre-exponential constants in reaction rate expressions
B temperature dependent constant in reaction rate expression
c_p specific heat capacity
C_a agglomeration rate constant
C_{min} Number of carbon atoms in the incipient carbon particle
C_2 Planck's second constant
E activation energy
f_g gas phase mixture fraction
f_v soot volume fraction
H total enthalpy
h_{fi}^o heat of formation of species i
k Boltzmann constant, Arrhenius reaction rate
N_A Avogadros' number
N_c soot particle number density
p pressure
Q_{rad} radiative heat flux
r radial coordinate, reaction rates associated with soot reaction
R_o initial fuel radius of thermal element
$\bar{R}$ universal gas constant
S source term in the conservation equation
t time
T temperature
u velocity
Y mass fraction
W molecular weight

Greek Symbols

μ dynamic viscosity
ρ density
σ Stefan-Boltzmann constant
ϕ dependent variable
$\dot{\omega}_f$ reaction rate associated with fuel
σ_ϕ Schmidt/Prandtl number
ς fuel dependent radiative constant

Subscripts

f fuel
c associated with soot
cfo associated with soot generation
cox associated with soot oxidation
t total
th thermophoretic
∞ radiative environment conditions

INTRODUCTION

Fire propagation is driven by the coupling of heat and mass transfer processes between the gaseous and the condensed phases. A significant portion of the heat transfer rate is provided by radiative heat transfer mechanisms, of which soot radiation contributes significantly for many flames. Although time history effects are suspected to affect the dynamics of soot evolution

within heavily sooting non-premixed flames, the majority of soot chemistry calculations have been conducted for steady flame configurations.

Detailed computations of soot evolution have been presented by Frenklach et al. (1984). However, it is presently computationally prohibitive to simulate most reacting flow fields with the level of chemical sophistication detailed in their study. More typical in the way of studies on soot chemistry influences on combustion are investigations by Syed et al. (1990), Kennedy et al. (1990), Leung et al. (1991), Fairweather et al. (1992), and Sivathanu and Gore (1994). Syed et al. (1990) investigated soot formation and radiation in laminar flames and also in buoyant turbulent flames using a flamelet based model. The soot model used in that study was based upon models presented by Moss et al. (1988) where the rate expressions for soot formation were taken from laminar flame experiments. The temperature and gas species were specified by state relations. Kennedy et al. (1990) studied soot formation processes in a jet diffusion flame using a conserved scalar formulation to specify the major gas species and soot generation and destruction processes also specified as functions of the conserved scalar. Leung et al. (1991) detailed a four step soot formation model which was used with a detailed gas phase kinetics model to simulate ethylene and propane flames. Fairweather et al. (1992) modeled a methane air jet flame using the soot reaction mechanism of Leung and coworkers (1991) and a conserved scalar/PDF method for the gas species and temperature. Sivathanu and Gore (1994) examined a jet diffusion flame using a similar soot evolution model as Fairweather et al. (1992), but for higher sooting acetylene flames.

In this study, the combustion processes for a spherical diffusion flame element are computed. The soot mechanism is taken from Fairweather et al. (1992). The mechanism incorporates the effects of soot nucleation, surface growth, oxidation and agglomeration processes. Two methods are used to simulate the major gas species distributions. In the first method, the state relationship data taken from Gore (1986) are used to characterize the major gas species in terms of a gas-phase mixture fraction. A computational formulation similar to that of Sivathanu and Gore (1994) is used to compute the unsteady combustion process. In the second method, a single-step, finite-rate, chemical reaction mechanism is used to compute the species distributions. The mechanism used is for acetylene-air flames and is taken from Westbrook and Dryer (1981). Results of the unsteady element calculations are compared using both formulations, and similarities and differences between these calculations are noted and discussed.

PROBLEM FORMULATION

The diffusion flame is computed within a spherically symmetric fuel-air element. The equations governing the reaction process are

$$\frac{\partial\left(\rho_t r^2\phi\right)}{\partial t}+\frac{\partial\left(u\rho_t r^2\phi\right)}{\partial r}=\frac{\partial}{\partial r}\left(r^2\frac{\mu}{\sigma_\phi}\frac{\partial\phi}{\partial r}\right)+S_\phi r^2$$

with the following boundary conditions

$$\frac{\partial\phi}{\partial r}=0 \qquad @\ r=0$$

$$\frac{\partial\phi}{\partial r}=0 \qquad \text{as } r\rightarrow\infty$$

; ϕ represents the variables listed in Table 1. Mathematically, initial conditions for this system were provided in terms of the dependent variables to be solved. Physically, a gaseous fuel sphere was initially surrounded by air and a small premixed region at a sufficiently high ignition temperature was used to ignite the mixture. The ideal gas assumption is used for gaseous species and the pressure is assumed to be constant in both space and time.

For the soot mass fraction and soot particle number density equations, the velocity includes a thermophoretic component which is given by (Talbot et al., 1980).

$$u_{th}=-0.55\frac{\mu}{\rho_t T}\frac{\partial T}{\partial r}$$

State Relationship

Under the laminar flamelet concept there exists an one to one functional relationship between gas-phase mixture fraction and species concentration independent of the measurement location within the flame. The dependent variables include gas-phase mixture fraction f_g (defined as the fraction of the local material which was originally fuel species and is in gaseous phase), gas-phase total enthalpy $H=\sum\left(\int_{T_0}^{T}c_{pi}dT+h_{fi}^{o}\right)Y_i$, soot mass fraction Y_c and soot particle number density N_c. The viscosity μ, is a function of temperature and σ_ϕ are Prandtl/Schmidt numbers. The source terms for each dependent variable are presented in Table 1.

Table 1. The source terms and Prandtl/Schmidt Numbers for state relationship formulation

Variables	S_ϕ	σ_ϕ
f_g	$-S_{cfo}+S_{cox}$	0.7
H	$Q_{rad}-\frac{W_f}{2W_c}S_{cfo}h_{ff}^{o}+\frac{W_{co}}{W_c}S_{cox}h_{fco}^{o}$	0.7
Y_c	$S_{cfo}-S_{cox}$	500.
N_c	$r_{iv}-r_v\rho_t^2W_c^{-1/6}Y_c^{1/6}N_c^{11/6}$	500.

where

$$S_{cfo}=r_iW_c+r_{ii}\rho_tW_c^{1/3}Y_c^{2/3}N_c^{1/3}$$

$$S_{cox}=r_{iii}\rho_tW_c^{1/3}Y_c^{2/3}N_c^{1/3}$$

are source/sink terms due to soot formation, nucleation, and oxidation. The source/sink terms for N_C represent nucleation and agglomeration. The soot reaction rate parameters (i.e., r_i, r_{ii}, r_{iii}, r_{iv}, r_v) are discussed in the soot kinetics section (Fairweather et al.., 1992)..

The gas-phase mixture fraction is not a conserved scalar. The soot formation from the gaseous species reduces the gas-phase mixture fraction and the oxidation of the soot into gaseous species increases the gas-phase mixture fraction. Consequently, the source terms in the gas-phase mixture fraction equation are the same as those in the soot mass fraction equation but with the opposite sign. The source terms in the total enthalpy equation include a term due to radiation and the two chemical energy terms corresponding to the sources in the gas-phase mixture fraction equation. The formation of the soot from the fuel reduces the gas-phase chemical energy, the oxidation of soot into gaseous species (CO) tends to increase the gas-phase chemical energy.

One-Step Reaction Mechanism

An one-step reaction mechanism for acetylene taken from Westbrook and Dryer(1981) is employed in this study. The reaction rate equation has the form of

$$\dot{\omega}_f = A_1 \exp\left(-\frac{E_a}{RT}\right) Y_f^{a_1} Y_{o_2}^{b_1} \rho^{a_1+b_1} W_f^{1-a_1} W_{o_2}^{-b_1}$$

The constants are listed in Table 2.

Table 2. The one-step reaction constant of acetylene
Units are cm-sec-mole-kcal-k(Westbrook and Dryer, 1981)

A	a_1	b_1	E_a
6.5E+12	0.5	1.25	30.0

The dependent variables to be solved include C_2H_2, CO_2, H_2O, CO, O_2, H_2, soot (C), soot particle number density and gas-phase total enthalpy. The source terms for all computed variables are listed in Table 3.

Table 3. Source terms and Prandtl/Schmidt Numbers
for one-step reaction mechanism

Variables	S_ϕ	σ_ϕ
Y_f	$-\dot{\omega}_f - \frac{W_f}{2W_c} S_{cfo}$	0.7
Y_{o_2}	$-\frac{2.5W_{o_2}}{W_f}\dot{\omega}_f - \frac{0.5W}{W_c} S_{cox}$	0.7
Y_{co}	$\frac{W_{co}}{W_c} S_{cox}$	0.7
Y_{co_2}	$\frac{W_{co_2}}{W_f}\dot{\omega}_f$	0.7
Y_{H_2o}	$\frac{W_{H_2o}}{W_f}\dot{\omega}_f$	0.7
Y_{H_2}	$\frac{W_{H_2}}{2W_c} S_{cfo}$	0.7
Y_c	$S_{cfo} - S_{cox}$	500.
N_c	$r_{i\upsilon} - r_\upsilon \rho_f^2 W_c^{-1/6} Y_c^{1/6} N_c^{11/6}$	500.
H	$Q_{rad} - \frac{W_f}{2W_c} S_{cfo} h_{ff}^o + \frac{W_{co}}{W_c} S_{cox} h_{fco}^o$	0.7

The source terms for soot mass fraction, soot particle number density and gas phase total enthalpy are the same as in the state relationship formulation.

Soot Kinetics Mechanism

The soot kinetics mechanism includes soot nucleation, surface growth, oxidation and particle coagulation steps (Leung et al., 1991, Fairweather et al., 1992). In this reduced soot model, the pyrolysis product, acetylene, not necessarily the fuel itself, is of primary importance in the soot formation. The model can either be combined with detailed chemistry (Leung et al., 1991) or incorporated into a reduced chemical reaction mechanism. By employing the 4-step soot kinetics and laminar flamelet (equilibrium) assumption, Sivathanu and Gore (1994) solved the gas-phase mixture fraction and enthalpy, soot mass fraction and soot particle number density equations in a laminar jet acetylene/air diffusion flame to examine the coupling effects of the soot and radiation. Fairweather et al. (1992) included the 4-step soot kinetics mechanism in computations of a turbulent jet diffusion flame in cross wind; they incorporated state relationship data taken from CH_4/air counter-flow diffusion flame measurements. The soot reaction rate terms of Fairweather et al., (1992) are employed in this work and are listed in Table 4.

Table 4. Reduced Soot Kinetics
of Fairweather et al. (1992)

$$r_i = k_i \rho_t W_f^{-1} Y_f$$
$$r_{ii} = k_{ii} f(p) \rho_t W_f^{-1} Y_f$$
$$r_{iii} = k_{iii} f'(p) \rho_t W_{o_2}^{-1} Y_{o_2}$$
$$r_{i\upsilon} = \frac{2}{C_{min}} N_A r_i$$
$$r_\upsilon = 2C_a \left(6W_{c(s)}/\pi\rho_{c(s)}\right)^{1/6} \left(6kT/\rho_{c(s)}\right)^{1/2}$$
$$f(p) = \pi\left(6W_{c(s)}/\pi\rho_{c(s)}\right)^{2/3}$$
$$f'(p) = f(p) / W_{c(s)}$$
$$k = AT^B \exp\left(-E/RT\right)$$

The Units of Rate Constants are kg, m, s, kmol, kcal, K

Rate Constant	A	B	E
k_i	1.35e+06	0.0	41000
k_{ii}	5.00e+02	0.0	24000
k_{iii}	1.78e+04	0.5	39000

C_{min} is the number of carbon atoms in the incipient carbon particle (9e+04), C_a is an agglomeration rate constant (3.0), N_A is Avogadros' number (6.022e+26 particles $kmol^{-1}$), k is the Boltzmann constant (1.381e-23 JK^{-1}), ρ_c is the soot density (2000kg m^{-3}), and W_c is the molar mass of soot (12 kg $kmol^{-1}$).

SOLUTION PROCEDURE

The source term due to radiation in the enthalpy equation is modeled as

$$Q_{rad} = -4a_p\sigma\left(T^4 - T_\infty^4\right)$$

where the Planck mean absorption is calculated to be

$$a_p = \frac{4\varsigma f_v T}{C_2}$$

where ς is a fuel dependent constant, C_2 is Planck's second constant and σ is Stefan-Boltzmann constant (Siegel and Howell, 1981). f_v is soot volume fraction. The radiative environment temperature is specified to be T_∞.

The conservation equations are nondimensionalized and are then solved by a control volume finite-difference scheme. The velocity is obtained from the conservation of mass equation. The gas-phase density is obtained from the equation of state. The total density (gas phase and soot) is obtained by a local homogeneity assumption. In the case of the state relationship formulation, the gas-phase mixture fraction, soot mass fraction, soot particle number density, total enthalpy, continuity and equations of state are solved iteratively for each time step. The gas species mass fractions are interpolated from the experimental data of Gore (1986) at each iteration. In the one-step reaction formulation, nine species mass fraction equations plus the equation of state and continuity are solved iteratively at each time

step. The reaction rates change by several orders of magnitude immediately after the ignition process. To obtain a converged solution, the time step in the one step reaction case has to be adjusted according to the reaction rate magnitude. The criteria for the convergence of all dependent variables at each time step is chosen as

$$\left| \frac{\phi_j^{old} - \phi_j^{new}}{\phi_j^{old}} \right|_{max} \leq 10^{-4}$$

RESULTS AND DISCUSSION

The discussion will first consider the global differences between the single step mechanism formulation and the state relationship formulations and then will consider the detailed local similarities and differences between the two formulations.

The flame trajectory computed from the state relationship differs from that computed by the finite rate chemical mechanism. In particular, for the low radiative-environment temperature cases, the differences are much greater than for high radiative-temperature conditions. The flame trajectory was computed using two criteria for the determination of the flame location. For the state relationship computations, the flame location is specified in terms of the stoichiometric mixture fraction value, and also in terms of the maximum temperature. For the finite rate computations, the flame location is calculated by finding the peak heat release rate value. In figure 1, the flame trajectory is compared for the finite rate computations and for the state relations computations. It is noted that the nondimensional time associated with fuel burnout is 14% shorter for the state relationship computation as compared with the finite rate computation for a case in which the initial fuel radius is 5mm and the radiative-environment temperature is 1000 K. It is also apparent that the significant deviation between the two trajectories occurs only after the flame has reversed its direction of propagation and intersects the soot shell which has followed the flame sheet on the fuel side. In figure 2, the mass consumption rate for the two sets of computations is shown. The consumption rate for the state relationship calculation is initially slightly larger than the mass consumption rate for the finite rate calculations which implies that the reaction process is chemically limited (i.e., the diffusion rate is larger than the chemical consumption rate). At a nondimensional time of 2, the mass consumption rate for the one step reaction becomes larger than the rate for the state relationship calculations. In general, as the mass of fuel decreases, the diffusion rate also decreases. For the state relationship calculation the rate of fuel mass consumption is specified solely by the diffusion rate. While for the finite rate calculations, a reaction Damkohler number contains all specifications of the rate of fuel consumption (i.e., a chemistry rate -diffusion rate balance).

For large radiative environment temperatures, the divergence of the radiative heat flux vector is small enough in the soot shell that there is not a significant disturbance to the reaction zone as the flame sheet passes through the soot shell, and for these conditions the flame sheet trajectories for the two formulations are similar. Finally it is seen that a pseudo-quenching process may be interpreted from the state relationship flame trajectory. This process is shown in figure 3 in which the flame trajectory for the state relationships calculation is computed using the value of the stoichiometric mixture fraction and also the value of the maximum temperature. For the high radiative temperature simulation, the curves for the flame trajectory by both methods are identical.

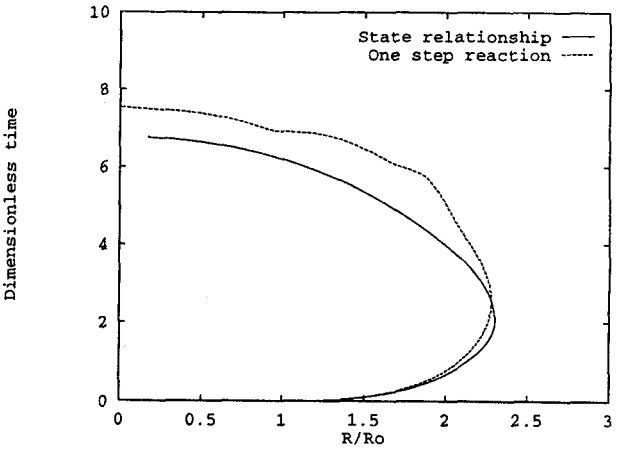

Figure 1. Flame trajectory for finite rate as compared with state relationship R_O=5mm, T_∞=1000K.

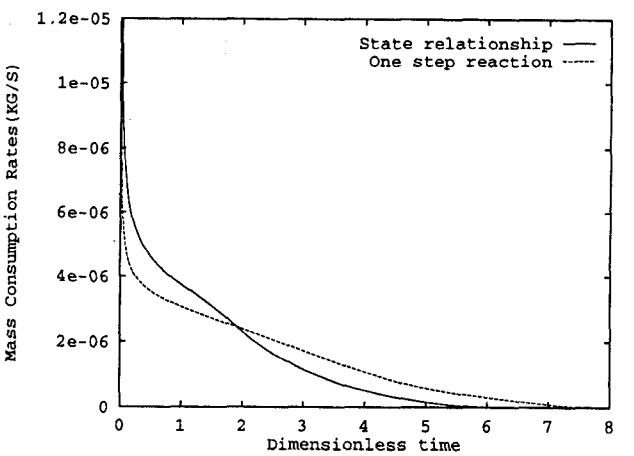

Figure 2. Comparison of mass consumption rates between one step and state relationship calculation.

For the high loss (low radiative temperature) simulation a deviation in the flame trajectory by the two methods occurs at a nondimensional time of approximately 6. This deviation may be interpreted as a type of quenching behavior (Ezekoye & Zhang, 1995). From the finite rate calculations it was found that flame quenching occurred for the low radiative temperature cases.

Although state relationships have been experimentally determined for a range of conditions, it was unclear what the effects of computationally determining these relations would be. The state relationships were extracted from the computational results and it was found that the major gas species using a single step mechanism collapsed into a global relation independent of the time at which the particular "measurement" was made. It was found that the apparent mixture fraction was the correct variable under which the global collapse would occur. The presence of any significant soot mass fraction makes both the total mixture fraction and the gas phase mixture fraction inappropriate independent variables. The species distributions for acetylene, oxygen, water, carbon dioxide and nitrogen as determined by the finite rate calculation are presented in figure 4.

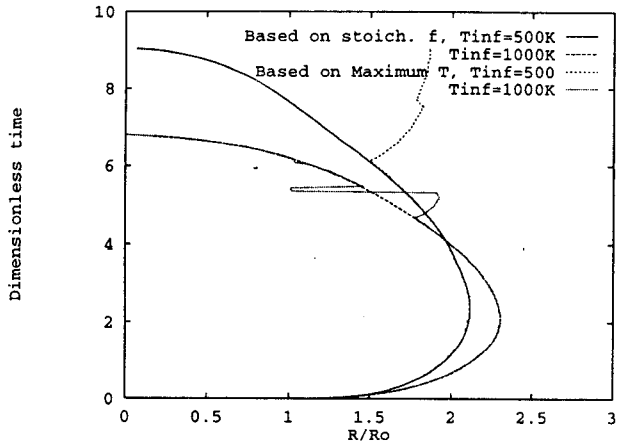

Figure 3. Flame trajectories for state relationship simulation for different environmental temperatures.

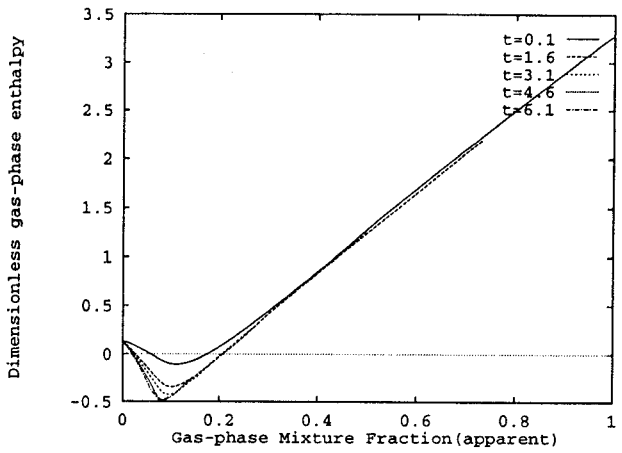

Figure 5. The state relationship for gas-phase total enthalpy obtained from one step reaction mechanism.

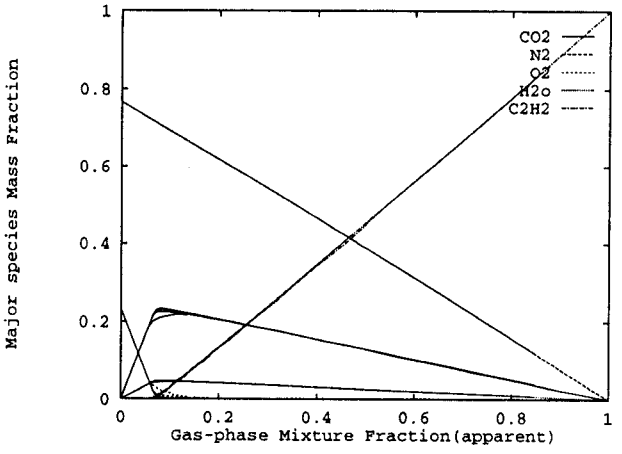

Figure 4. Major gas species state relationships computed using one step reaction mechanism.

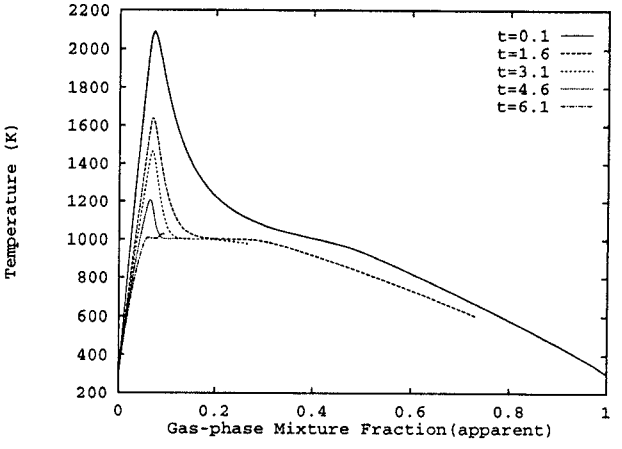

Figure 6. Temperature profile in mixture fraction space for R_O=5mm and T_∞=1000K.

The gas phase total enthalpy distribution is shown in figure 5. An universal relationship is found for this parameter when it is plotted in the apparent gas phase mixture fraction space. Small deviations in the universality of the profile are found in a small mixture fraction range near the stoichiometric value. These deviations are primarily due to radiative transfer from the soot species. The distortion of the curve from universality appears even slightly on the oxygen side of the flame sheet implying that diffusive effects to the soot shell are important in this region. This trend was observed by Jang (1992) for a steady acetylene jet diffusion flame calculation in which the major gas species were determined from state relationship data and the soot profiles were specified by using experimental data/profiles. The temperature distribution is shown in figure 6 for a radiative environment temperature of T_∞=1000K . At early times the peak temperature is on the order of the adiabatic flame temperature. For all times the temperature gradient in mixture fraction space towards the soot shell is nearly constant on the fuel side of the flame, while its value on the air side continues to decrease with increasing time.

The relations for hydrogen and carbon monoxide are not universal/global. Errors are expected in the computed CO species distribution given that the chemical mechanism utilized was only one step and did not explicitly account for the fuel decomposition into CO; all CO generated in the finite rate computations is formed by soot oxidation reactions. It is well established that the soot species distribution does not follow a universal relation, as is shown in figures 7a and 7b (T_∞=1000K) for state relationship and one step calculation (at the same times) respectively. The magnitude of the peak soot volume fraction is similar for the two methods of computation (i.e., finite rate or state relationship). Soot volume fractions are strongly influenced by the radiative temperature. In figure 8, the soot volume fractions are shown for a series of times from the one step calculation for T_∞=500K. By comparing figure 7b and 8, it can be seen that the peak soot volume fraction is consistently larger for the low radiative temperature (high heat loss cases). Several effects appear to contribute towards this observation. The first effect is that the total time for the high radiative temperature simulation is shorter than that for the low temperature case.

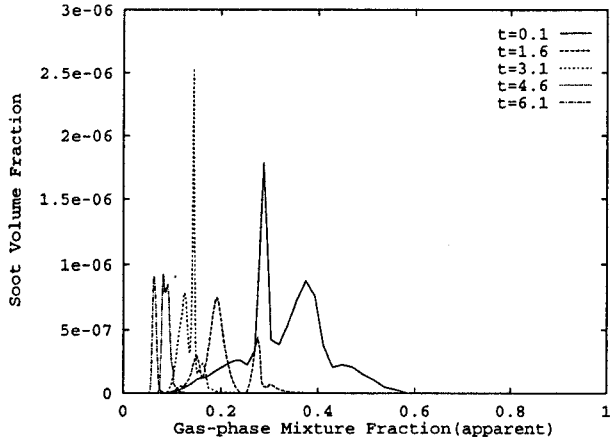

Figure 7a. Soot volume fraction profiles computed using state relationships for T_∞=1000K.

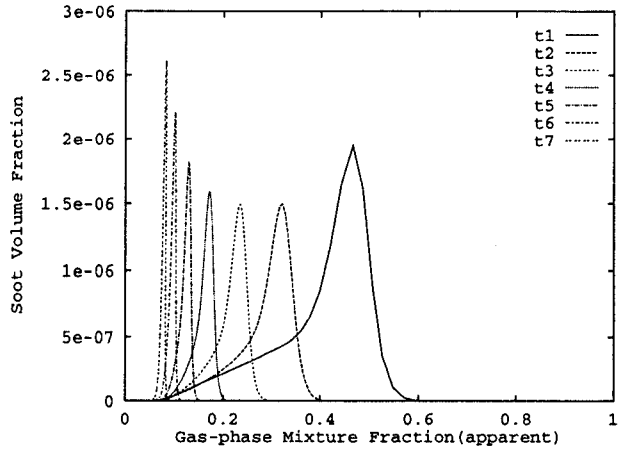

Figure 8. Soot volume fraction profiles computed using one step reaction mechanism for T_∞=500K.

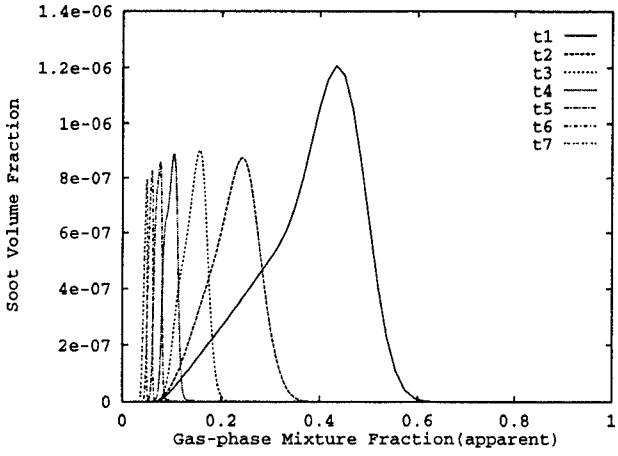

Figure 7b. Soot volume fraction profile computed using one step reaction mechanism for T_∞=1000K.

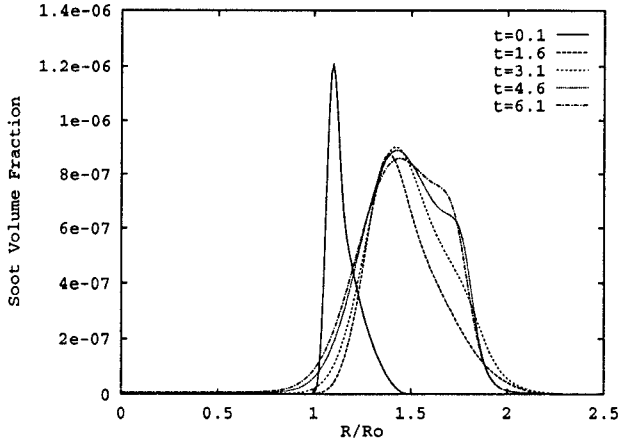

Figure 9. Soot volume fraction profiles in physical space computed using one step reaction mechanism for T_∞=1000K.

Thus, there is longer time for soot reactions to occur. It is important to note that soot oxidation rates are generally smaller than the generation rates at earlier times. The second effect is that the activation energy for the soot surface growth reaction is significantly smaller than that for the fuel pyrolysis reaction, thus favoring soot growth at relatively low temperatures. This can be confirmed by specifically focusing on late times for the low radiative temperature problem in which the primary fuel consumption reaction has been quenched, while soot production and growth continue to occur. Although the soot distribution appears to be widely distributed in mixture fraction space, it is seen in figure 9 that the distribution for all times is generally narrowly centered in physical space. The reaction rates associated with the soot mechanism of Leung et al.(1991) and Fairweather et al.(1992) were compared with those generated by Sivathanu and Gore (1994). The reaction rates compare favorably, and it was found that the greatest sensitivity to these reaction rates was associated with the radiative environment temperature.

Radiative quenching becomes possible when the soot shell begins to interact with the flame sheet. The net radiative losses and the chemical heat release are shown in figures 10a and 10b as a function of time for state relationship and one step reaction simulations respectively. For finite rate chemistry and the radiative temperature case of T_∞= 1000K the net losses never exceed the chemical heat release rate (fig. 10a), while for the radiative temperature case of T_∞= 500 K the net losses exceed the chemical heat release rate at a nondimensional time of approximately 9. For the state relations calculations, the crossover occurs for both radiative temperature cases of T_∞= 500K and 1000K (fig. 10b). These crossovers occur at approximately 4 to 5 nondimensional time. The criteria for transient quenching is somewhat more complicated than a simple balance of total losses to net release; such a criteria has been established by Ezekoye and Zhang (1995) for transient diffusion flame quenching phenomena.

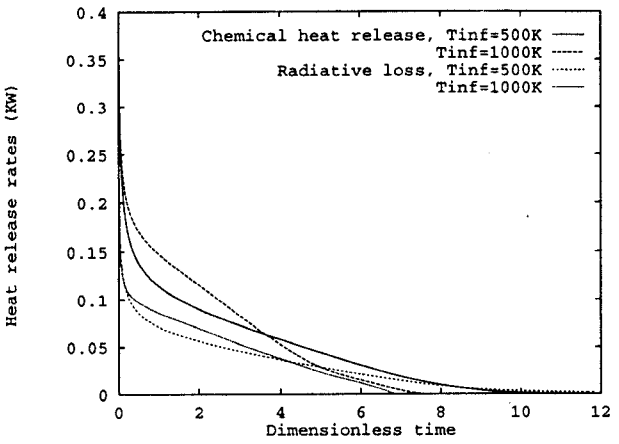

Figure 10a. Heat release rates and radiative loss rates from one step reaction simulation.

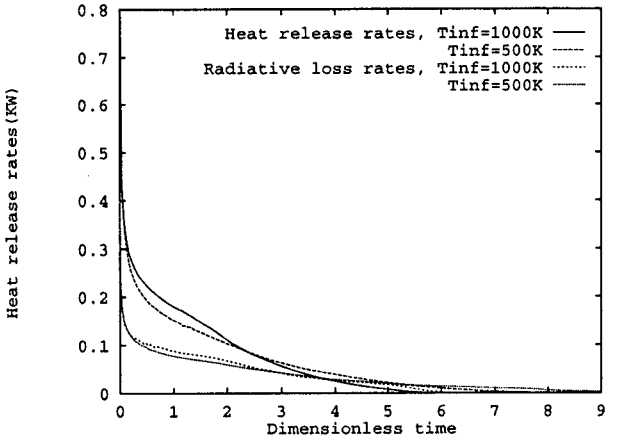

Figure 10b. Heat release rates and radiative loss rates from state relationship simulation.

The size of the fuel core of the thermal element was not found to significantly alter the above results. It was noted that the nondimensional time for fuel burnout was slightly increased for a larger initial radius fuel core consistent with Zhang and Ezekoye (1994). It was also found that the soot shell was the same size in mixture fraction space for an initially larger fuel core element. The total amount of soot was increased and the peak soot volume fractions were increased due to the longer physical time available for soot growth processes.

CONCLUSIONS

In this study, the combustion processes for a spherical acetylene-air diffusion flame element using computed using two different approaches. In the first case, generalized state relations are used to specify the major gas species distributions, while in the second case, a finite rate reaction mechanism is used. A simplified soot mechanism which incorporates the effects of soot nucleation, surface growth, and agglomeration processes was used to specify the soot species evolution. It was found that as the net radiative losses for the diffusion flame element approaches zero, the predictions of the state relations match those of the finite rate chemistry calculations. Computationally derived generalized state relationships were found to collapse the major species within the flame, although minor species deviate at large net radiative loss fractions.

Acknowledgments: This work is supported by the National Institute of Standards and Technology (NIST) under Grant No. 60NANB3D1436.

REFERENCES

Ezekoye, O. A. and Zhang, Z., "Modeling of a Lagrangian Flamelet with Radiation Interaction", Combustion Science and Technology, in press 1995.

Fairweather, M., Jones, W. P., and Lindstadt, R. P., "Predictions of Radiative Transfer from a Turbulent Reacting Jet in a Cross-Wind", Combustion and Flame, 89, 1992.

Frenklach, M., Clary, D.W., Gaediner, W. C., and Stein, S. E., "Detailed Kinetic Modeling of Soot Formation in Shock-tube Pyrolysis of Acetylene," Twentieth Symposium (International) on Combustion/The Combustion Institute, p. 887, 1984.

Gore, J. P., "A Theoretical and Experimental Study of Turbulent Flame Radiation", Ph.D. Thesis, The Pennsylvania State University, State College, PA, 1986.

Jang, J. H., "Transient Radiation Properties of Strongly Radiating Turbulent Flames", Ph.D. dissertation. University of Maryland, College Park, MD, 1992.

Kennedy , I. M., Kollmann, W., and Chen, J. Y., "A Model for Soot Formation in a Laminar Diffusion Flame", Combustion and Flame, Vol. 81, pp.73-85, 1990.

Leung, K. M., Lindstedt, R. P., and Jones, W. P, "A Simplified Reaction Mechanism for Soot Formation in Nonpremixed Flame", Combustion and Flame Vol. 87, pp.289-305, 1991.

Moss, B.J., Stewart, C.D., and Syed, K. J., "Flowfield Modeling of Soot Formation at Elevated Pressure", Twenty-Second Symposium (International) on Combustion/The Combustion Institute, pp. 413-423, 1988.

Siegel, R. and Howell, J. R., Thermal Radiation Heat Transfer, Hemisphere Publishing Company, 1981.

Sivathanu, Y. R. and Gore, J. P., " Coupled Radiation and Soot Kinetics Calculations in Laminar Acetylene/Air Diffusion Flames," Combustion and Flame, 97, 1994.

Syed, K. J., Stewart, C.D., and Moss, J. B., " Modeling Soot Formation and Thermal Radiation in Buoyant Turbulent Diffusion Flames," Twenty-Third Symposium (International) on Combustion/The Combustion Institute, pp. 1533-1541, 1990.

Talbot, L., Cheng, R. K., Schefer, R. W., and Willis, D. R., "Thermophoresis of Particles in a Heated Boundary Layer", J. Fluid Mechanics, Vol. 101, pp. 737-758, 1980.

Westbrook, C. K. and Dryer, F. L., "Simplified Reaction Mechanisms for the Oxidation of Hydrocarbon Fuels in Flames", Comb. Sci. and Tech., Vol. 27, pp. 31-34, 1981.

Wichman, I. S., " On the Influence of a Fuel Side Heat-Loss ('Soot') Layer on a Planar Diffusion Flame," Combustion and Flame, 97, 1994.

Zhang, Z and Ezekoye, O.A., " Combustion of a Thermal Element in a Radiative Field", HTD-Vol. 296, Fire, Combustion and Hazardous Waste Processing, ASME 1994.